Commun Nonlinear Sci Numer Simulat 89 (2020) 105288

Contents lists available at ScienceDirect

Commun Nonlinear Sci Numer Simulat

journal homepage: www.elsevier.com/locate/cnsns

Research paper

Freak chimera states in a locally coupled Duffing oscillators chain

M.G. Clerc [a], S. Coulibaly [b], M.A. Ferré [a,*]

[a] Departamento de Física and Millennium Institute for Research in Optics, Facultad de Ciencias Físicas y Matemáticas, Universidad de Chile, Casilla 487-3, Santiago, Chile
[b] Univ. Lille, CNRS, UMR 8523 - PhLAM - Physique des Lasers Atomes et Molécules, F-59000 Lille, France

ARTICLE INFO

Article history:
Received 18 September 2019
Revised 7 April 2020
Accepted 9 April 2020
Available online 13 April 2020

Keywords:
Coupled nonlinear oscillators
Chimera states
Localized structures

ABSTRACT

Arrays of oscillators driven out-of-equilibrium can support the coexistence between coherent and incoherent domains that have become known as chimera states. Recently, we have reported such an intriguing self-organization phenomenon in a chain of locally coupled Duffing oscillators. Based on this prototype model, we reveal a generalization of chimera states corresponding to the coexistence of incoherent domains. These freak states emerge through a bifurcation in which the coherent domain of an existing chimera state experiences an instability giving rise to another incoherent state. Using Lyapunov exponents and Fourier analysis allows us to characterize the dynamical nature of these extended solutions. Taking the Kuramoto order parameter, we were able to compute the bifurcation diagram of freak chimera states.

1. Introduction

Coupled oscillators usually exhibit synchronization phenomenon [1] making all oscillators to move in a well-coordinated manner. In the last decade, coexistence between coherent and incoherent domains in an array of identical oscillators has attracted the attention of the scientific community [2]. This intriguing dynamical behavior has been called a chimera state. Pioneering studies of these states were conducted on a lattice of chaotic maps globally coupled [3] and an array of phase-oscillators with weak nonlocal coupled [4]. Since then, chimera states were theoretically studied in more general frameworks, such as coupled phase oscillator models [5–7], coupled maps networks [8–10], array of nonlinear oscillators [11–15], array of chaotic systems [16–19], quantum systems [20], neural models [21,22], delay systems [23,24], and discrete metamaterials [25]. Chimera states have been experimentally observed and investigated in a chemical system [26,27], optoelectronic oscillators [28,29], mechanical oscillator networks [30,31], electric circuit [32,33], and lasers [34,35]. Recently, chimera states have been numerically observed in a Duffing oscillators chain coupled to nearest neighbors [36]. The local coupling prevents the incoherent domain from invading the coherent one, allowing concurrently the existence of a family of chimera states, which are organized by a homoclinic snaking-like bifurcation diagram [37,38]. The effect of the local coupling on domain dynamics can be modeled considering the Peierls-Nabarro potential [39–41]. Indeed, this potential accounts for the energy barrier that establish the coexistence between the coherence and incoherence domains. Hence, it is expected that increasing the energy injection one domain invades the other one. Namely, the chimera solution changes in size or becomes unstable.

* Corresponding author.
E-mail address: mferre@ing.uchile.cl (M.A. Ferré).

https://doi.org/10.1016/j.cnsns.2020.105288
1007-5704/

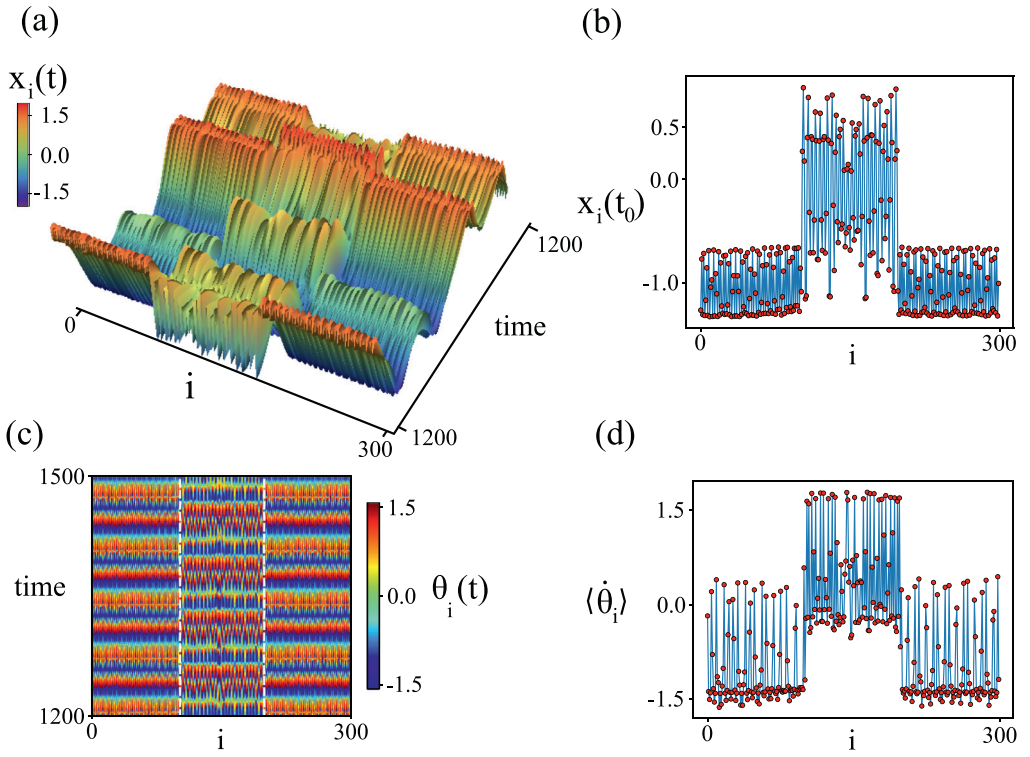

Fig. 1. Freak chimera state of the Duffing oscillators chain coupled to nearest neighbors Eq. (1) by $\alpha = 0.4$, $\beta = 1.0$, $\mu = 0.1$, $\omega = 0.7$, $N = 300$, $\gamma = 2.8$, and $\kappa = 0.5739$. (a) Spatiotemporal evolution of one freak chimera state. (b) Instantaneous profile of chimera state a fixed given time. (c) Spatiotemporal diagram of the phase of each oscillator, $\theta_i \equiv \arctan(\dot{x}_i/x_i)$. (d) Average frequency of each oscillator, $\langle \dot{\theta}_i \rangle \equiv \int_0^T \dot{\theta}_i(t)dt/T$.

However, this scenario can be altered if one of the domains suffers an instability. When the coherent state exhibits an instability, leading to a new complex domain, one may observe the coexistence of incoherent states of different nature. This type of dynamical behavior corresponds to a generalization of the chimera state.

This work aims to investigate coexistence between incoherent domains in a Duffing oscillators chain with the nearest neighbor coupling scheme. We have termed these intrigued states as *freak chimera states*. The dynamical nature of these extended solutions is characterized by Lyapunov exponents and Fourier analysis. A bifurcation diagram of the different states is presented. We also propose a quantitative measure of the difference between chimera and freak chimera states based on the local and global Kuramoto order parameter. Hence, we were able to identify that the freak chimera states emerge as a supercritical bifurcation of the chimera states, in which the coherent domain becomes unstable by a modulational instability.

2. Duffing oscillators chain and freak chimera states

Let us consider a chain of N locally coupled Duffing oscillators that satisfies

$$\ddot{x}_i(t) = -x_i + \alpha x_i^3 - x_i^5 - \mu \dot{x}_i + \gamma \cos \omega t + \kappa \left(x_{i+1} - 2x_i + x_{i-1} \right), \tag{1}$$

where $x_i(t)$ accounts for the displacement of the ith-oscillator with a unitary natural frequency. Oscillators are indexed by $i = \{1, 2, \ldots, N\}$. The nonlinear terms characterize the stiffness, and μ accounts for the damping coefficient. A harmonic forcing provides the injection of energy with amplitude and frequency γ and ω, respectively. The coupling between oscillators is modeled using a linear spring of elastic constant κ.

The Duffing oscillator is a prototype model for the resonance phenomenon in out of equilibrium systems [42]. Model Eq. (1) exhibits dissipative structures such as standing waves, spatiotemporal chaos, extended quasi-period oscillations, chimera states, among other behaviors [36]. These chimera states are characterized by the coexistence of coherent and incoherent domains in a unidimensional (1D) lattice coupled-oscillators. Increasing the amplitude of forcing, the coherent domain of the chimera state becomes unstable giving rise to a state that presents coexistence between two incoherent domains. We have termed these solutions as freak chimera states. Fig. 1 shows a typical spatiotemporal evolution freak chimera state observed in model Eq. (1) either considering the absolute displacement $x_i(t)$ (Fig. 1(a)) or the local phase (Fig. 1(c)). Typical instantaneous profiles are depicted in Fig. 1(b) and (d). It can be seen from the spatiotemporal diagrams in the variable $x_n(t)$ and phase $\theta_n(t) \equiv \arctan(\dot{x}_n/x_n)$ that all the distinct domains of the chimera exhibit complex behaviors. In chimera state, the frequency of the oscillators remains constant all over coherent domains. This frequency can be monitored introducing

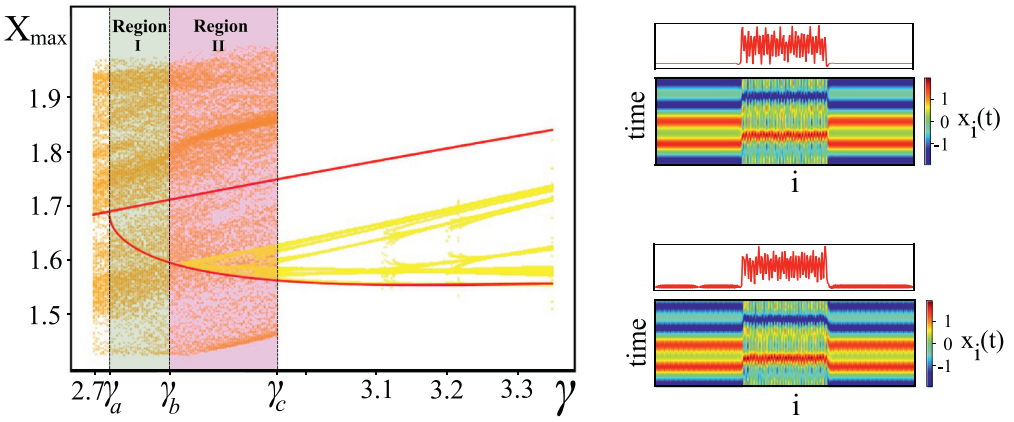

Fig. 2. Bifurcation diagram of the Duffing oscillators chain coupled to nearest neighbors model Eq. (1) by $\kappa = 0.4216$ and $\alpha = 0.4$. Maximum displacement $X_{\max}$ of each oscillator as a function of the amplitude of the forcing γ. The solid red lines depict the maximum displacement of limit cycles for a single Duffing oscillator. Orange and yellow squares represent $X_{\max}$ of each oscillator of the extended oscillatory solutions. The upper extended solution presents a spatiotemporal chaotic dynamics until $\gamma_c = 2.96131$. The lower extended solution appears by a saddle-node bifurcation at $\gamma_a = 2.7196$, which is an extended synchronized state that exhibits a modulation instability at $\gamma_b = 2.8143$. This instability causes the emergence of an extended state of quasi-periodic nature. Chimera and freak-chimera states are observed in I and II region, respectively. Insets illustrate, respectively, chimera and freak chimera state at $\gamma = 2.75$ and $\gamma = 2.83$. (For interpretation of the references to colour in this figure legend, the reader is referred to the web version of this article.)

the quantity $\langle \dot{\theta}_n \rangle \equiv \int_0^T \dot{\theta}_n(t) dt/T$, where T is an average time chosen several times larger than the period of the external forcing. Fig. 1(d) depicts $\langle \dot{\theta}_n \rangle$ for the freak chimera state, revealing a complex spatial structure for these states. Note that positive and negative frequency accounts for the clockwise and counterclockwise evolution of oscillators trajectories in the phase portrait, respectively. This allows us to highlight another difference between freak chimera and chimera states. Note that the profile of $\langle \dot{\theta}_n \rangle$ changes accordingly to T, as result of the complex spatiotemporal nature of the incoherent domains. Numerical simulations were conducted using a finite differences code with 4th-order Runge-Kutta scheme, with Neumann boundary conditions, and time step fixed as $dt = 0.01$. To obtain a chimera state, we consider an initial condition that connects the extended lower and upper states with a small spatially random perturbation [36].

3. Duffing oscillators chain dynamics

Chimera and freak chimera states are observed in the Duffing oscillators chain model Eq. (1) inside the bistable regime. Consequently, bistability is a prerequisite condition to observe these intriguing states. To shed light on the solutions and instabilities of the model Eq. (1), the maximum displacement of each oscillator is calculated and defined as $X_{\max}$. Fig. 2(a) illustrates $X_{\max}$ as a function of γ. For the sake of simplicity, we have first considered a single oscillator. The solid red line represents the maximum displacement of an individual Duffing oscillator. For small γ only one periodic solution is observed [36]. Notice that the maximum displacement increases as a function of the external forcing. At $\gamma_a = 2.7196$ a second limit-cycles emerges from a saddle-node bifurcation. From this γ_a, we observe bistability between two limit cycles. To distinguish between these limit cycles, we have introduced the following terminology upper and lower limit cycle according to the maximum displacements that they exhibit.

Let us considered the collective evolution of coupled limit cycles. From the numerical simulations, we observe that the collective behavior of the oscillators can be synchronized or not depending on parameters. The dynamical behaviors formed from the upper and lower oscillators are called, respectively, as upper and lower extended solutions. The maximum displacement $X_{\max}$ of these solutions are depicted by orange and yellow squares in Fig. 2, respectively. Notice that the upper extended solution is of complex spatiotemporal nature. This dynamic behavior persists until $\gamma_c = 2.96131$. At this critical value, the upper strange attractor suddenly disappear by a crisis [43]. Therefore, for $\gamma > \gamma_c$ the lower branch accounts for the only state that perseveres. On the other hand, the extended lower solution appears by a saddle-node bifurcation at $\gamma_a = 2.7196$. For $\gamma_a < \gamma < \gamma_b = 2.8143$, the lower extended solution is synchronized. In this interval, the maximum displacement of the lower extended solution decreases monotonously. Fig. 2 highlights this interval as region I. The lower extended solution suffers a modulation instability at γ_b. This instability gives rise to the emergence of new incoherent behavior for $\gamma > \gamma_b$ (cf. Fig. 2). Hence, for $\gamma_b < \gamma < \gamma_c$, the Duffing chain model (1) exhibits a coexistence between two incoherent dynamical behaviors. Therefore, in this region of coexistence of complex states, one expects to observe coexistence between two incoherent domains (see Fig. 1) producing freak chimera states. Insets in Fig. 2 depict a chimera and freak-chimera states at $\gamma = 2.75$, and $\gamma = 2.83$ respectively.

To characterize the spatiotemporal dynamics of the solutions observed in model Eq. (1), computation of Lyapunov spectra and Fourier analysis were conducted. The Lyapunov exponents characterize the exponential sensitivity to initial conditions of dynamical systems [44]. When the maximum Lyapunov exponent is negative, zero, or positive, the system shows

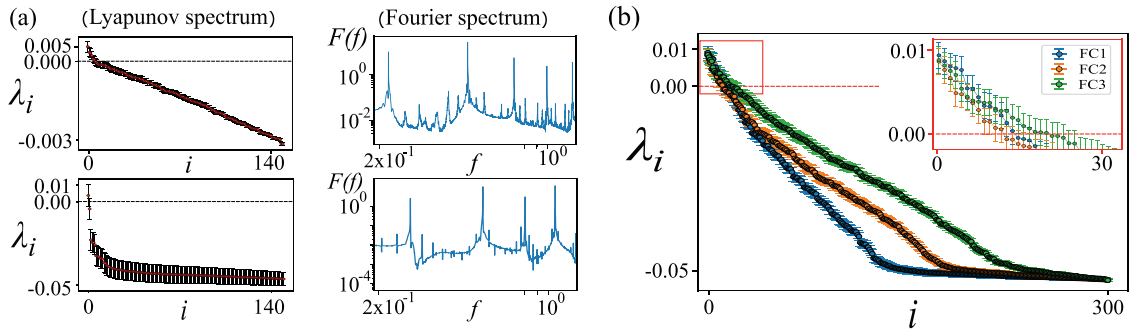

Fig. 3. Dynamical characterization of chimera states. (a) Lyapunov spectrum and Fourier analysis of the upper (top panels) and lower (bottom panels) extended state. The red dots account for the numerical Lyapunov exponents and the vertical bars account for their respective error. $F(f)$ accounts for the Fourier spectrum of the field $\zeta(t) = \sum_{i=1}^{N} |x_i(t) - x'_i(t)|$, where $x_i(t)$ and $x'_i(t)$ are solutions of Eq. (1) with slightly different initial conditions, for the extended upper and lower solutions. These plots exhibit the typical Fourier spectrum for chaotic and quasiperiodic solutions, respectively. (b) Lyapunov spectra of different freak-chimera states of 140, 200 and 250 size, respectively. FC1, FC2, and FC3, respectively, account for the different freak-chimera states. The inset shows an amplification around the larger Lyapunov exponents. (For interpretation of the references to colour in this figure legend, the reader is referred to the web version of this article.)

a stationary, oscillatory, and chaotic dynamics, respectively. A discrete set of positive Lyapunov exponents reveals a chaotic dynamical behavior of a low-dimensional dynamic system. Otherwise, a continuous set of positive Lyapunov exponents characterize the spatiotemporal chaotic evolution of the system under study. The analytical determination of Lyapunov exponents is inaccessible in general. A strategy to determine these exponents is through numerical calculation. Let us introduce the Lyapunov exponents λ_i, which are indexed by $i = \{1, 2, \ldots, 2N\}$. Lyapunov exponents are characterized according to their values as following $\lambda_1 \geq \lambda_2 \geq \ldots \lambda_{2N}$. Using the strategy proposed in Ref. [45], we have computed numerically Lyapunov spectra. Fig. 3(a) shows typical Lyapunov spectra for the upper and lower extended state. As it is expected, the upper extended state is characterized by several positive Lyapunov exponents. Hence, the upper extended state is of spatiotemporal chaotic nature. Likewise, to complement the characterization of the complex dynamic observed, a Fourier analysis is considered. Let us consider the difference between two solutions with slightly different initial conditions $x_i(t)$ and $x'_i(t)$, and introduce the field $\zeta(t) \equiv \sum_{i=1}^{N} |x_i(t) - x'_i(t)|$. Fig. 3(a) illustrates the Fourier spectrum of $\zeta(t)$ for the upper (top panel) and lower (bottom panel) extended solutions. From these charts, it can be observed that the upper and lower extended solutions exhibit the typical Fourier spectrum of a chaotic and quasi-periodic dynamical behavior, respectively. In addition, the lower extended state shows only one non-negative Lyapunov exponent. Due to the closeness to zero value and its error-bar of the largest Lyapunov exponent, we cannot conclude that this dynamical behavior corresponds to a chaotic one. Fourier analysis allows us to conclude that this dynamic behavior is of quasi-periodic nature. Indeed, the Fourier spectrum exhibits two immeasurable frequencies. In brief, in the region II of Fig. 2, the system presents the coexistence of spatiotemporal chaos and quasi-periodic dynamical behaviors.

To shed light on the dynamical nature of the freak-chimera states, we have calculated their Lyapunov spectrum. Fig. 3(b) shows the typical Lyapunov spectra of three different freak-chimera states with 140, 200, and 250 size, respectively. The size refers here to the number of oscillators inside the incoherent domain. Notice that for larger chimera states, the number of positive Lyapunov exponents increases. This highlights the spatiotemporal chaotic nature of the upper extended solution, and consequently, the spatiotemporal chaotic nature of freak-chimera states. Therefore, larger chimeras exhibit a more complex dynamic since they have a higher number of positive Lyapunov exponents.

4. The transition from chimera state to freak-chimera state

Chimera states become freak-chimera states when the lower extended solution develops incoherent dynamics. Indeed, these chimeras emerge as an instability of the background state (lower extended state) on which the chimera is held. Hence, the characterization of the transition of the lower extended state from coherent to incoherent evolution is necessary to reveal the emergence mechanism of the freak-chimera state. To characterize this transition, we have computed the global Kuramoto order parameter $R(t)$ given by:

$$R_N(t) = \frac{1}{N}\left|\sum_{n=1}^{N} e^{i\theta_n(t)}\right|, \tag{2}$$

where $\theta_n(t) \equiv \arctan(\dot{x}_n/x_n)$ accounts for the phase of the nth Duffing oscillator. The global Kuramoto order parameter characterizes the level of synchronicity of the oscillators chain. In a fully synchronized state, R_N is identical to one. Contrarily, in a full incoherence state, R_N is zero. Fig. 4(a) shows the temporal average of $R(t)$ for the lower extended, upper extended, and different chimera states. For $\gamma_a < \gamma < \gamma_b$, the value of the global order parameter of the lower extended solution is identical to one. This state is represented by the acronym LES in Fig. 4(a). Increasing the strength of the external forcing,

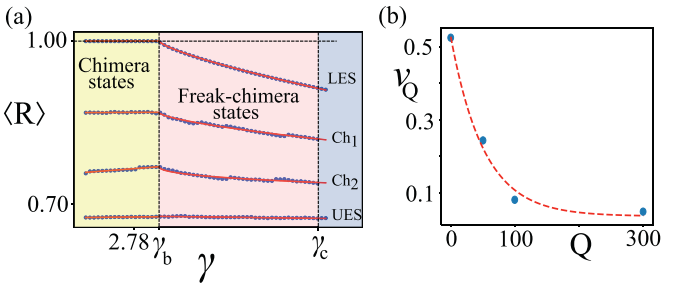

Fig. 4. The transition from chimera state to freak-chimera state. (a) Temporal Average of the global Kuramoto order parameter for different extended states. The symbols LES, UES, Ch_1 and Ch_2 account for lower extended, upper extended, and chimera states, respectively. (b) Power law exponent ν_Q as a function of the number of oscillators in the upper extended domain Q.

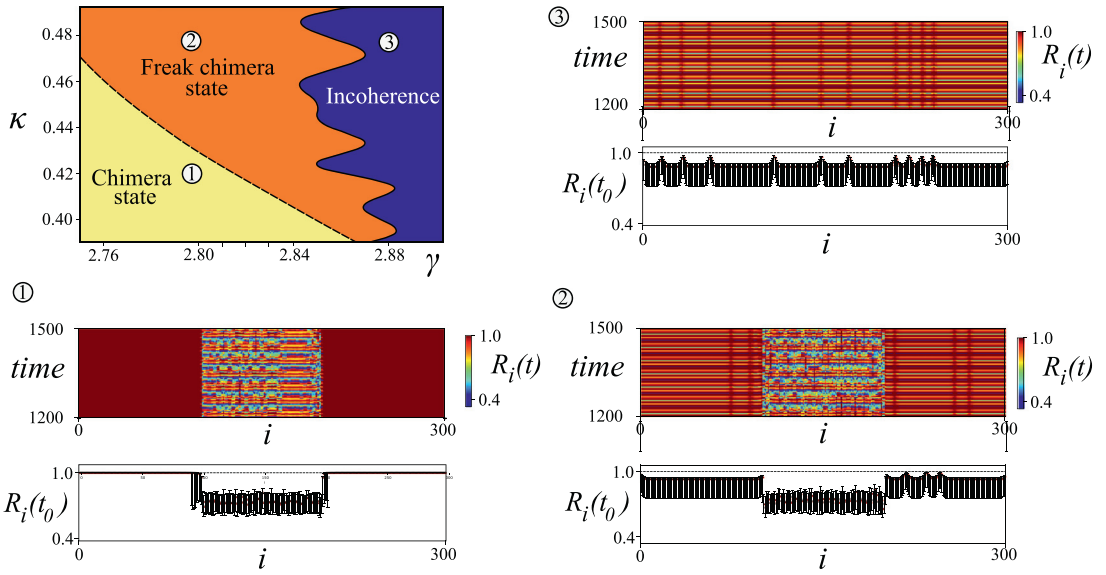

Fig. 5. Phase diagram of chimera and freak-chimera state in the coupling strength κ and the intensity of the external forcing γ. The dashed curve accounts for the transition between chimera and freak-chimera state. The solid line stands for the transition between freak-chimera and incoherent domain. Insets display the typical instantaneous profile and the spatiotemporal diagram of the local order parameter $R_i(t)$ of a chimera, freak-chimera, and extended incoherence state.

$\gamma_c > \gamma > \gamma_b$, this state exhibits an incoherent dynamics, $\langle R \rangle < 1$. From this chart, one concludes that the extended state exhibits a second-order transition. Close to this transition, the temporal average global Kuramoto order parameter $\langle R_Q \rangle$ of different freak-chimera state decreases following a power law given by:

$$\langle R_Q \rangle = r_0(\gamma - \gamma_b)^{\nu_Q}, \tag{3}$$

where r_0 and ν_Q are dimensionless constants, and Q accounts for the number of oscillators in the upper extended domain (chimera size). Fig. 4(b) shows ν_Q as a function of the number of oscillators in the upper extended domain. Note that ν_Q is a monotonically decreasing function with maximum value ν_0 close to 1/2. Besides, ν_0 corresponds to the critical exponent of the lower extended state. Note that the minimum value of ν_Q is observed for the upper extended state. Therefore, the transition from the chimera state to the freak-chimera state is of a second-order nature with a critical exponent that depends on the size of the chimera. From the freak-chimera states, when increasing the strength of the forcing γ, this state becomes unstable through a crisis giving rise to the only stable state, which corresponds to the incoherent extended state.

Thanks to the temporal average global Kuramoto order parameter, we can characterize in the parameter space the regions where the chimera states and the freak-chimera states are observed. Fig. 5 shows the phase diagram in (κ, γ)-plane, revealing a smooth transition between the chimera and freak-chimera states. Only chimera states were considered to obtain this phase diagram. The other steady-states that are present in the system can enrich this phase diagram; however, for the sake of simplicity, we focus on chimera states. Note that the transition between chimera and incoherent state is very complex, even expects it to be fractal.

The global Kuramoto order parameter quantifies the synchronization level of the entire system. However, this parameter is not able to distinguish the synchronization level of each domain. In order to characterize the synchronization level of

each domain, let us introduce the local order parameter

$$R_i(t) = \frac{1}{3}\left|\sum_{j=i-1}^{i+1} e^{i\theta_j(t)}\right|. \tag{4}$$

Insets in Fig. 5 depict spatiotemporal temporal evolution and profile of the local order parameter $\langle R_i \rangle$ of a chimera, freak-chimera, and extended incoherence state. As expected, the local order parameter in the coherence domain shows a constant value equal to one. Nevertheless, once this domain becomes unstable, R_i shows a finite number of spatial structures. These spatial structures correspond to synchronized defects, which are motionless due to the quasiperiodic nature of the lower extended solution. In brief, the local order parameter is the adequate quantity to characterize the different domains that constitute chimera and freak chimera states.

5. Conclusion

Based on a Duffing oscillators chain with nearest-neighbor coupling, we have revealed a generalization of chimera states that corresponds to coexistence between incoherent domains. Named as freak chimera states, they emerge as a bifurcation of the chimera state, in which the coherent domain suffers an instability and gives rise to an incoherent state. The prerequisite conditions of freak chimera states are the coexistence between two complex spatiotemporal temporal domains and an energy barrier that prevents the invasion from each other. In our particular case of the Duffing oscillators chain, both complex spatiotemporal behaviors emerge from two homogeneous periodic solutions that loose stability as the strength of the forcing increases. The energy barrier between incoherent domains emergence due to the discrete nature of the system. The strength of the coupling between oscillators controls the energy gap between the solutions, allowing the formation of localized solutions.

To characterize the spatiotemporal dynamics and dynamical nature of freak-chimera states, we have performed Fourier analysis and calculated the Lyapunov spectra of these localized states. The upper and lower extended solutions correspond to a spatiotemporal chaotic, and quasiperiodic one. Besides, based on the Kuramoto order parameter, the bifurcation diagram of chimera states is established. The transition between chimera and freak chimera states corresponds to a supercritical bifurcation.

Due to the perquisites for observing freak chimeras are quite general, we expect to observe this intriguing phenomenon in various coupled oscillators in mechanical, magnetic, optical, and chemical reaction systems.

Declaration of Competing Interest

The authors declare that they have no known competing financial interests or personal relationships that could have appeared to influence the work reported in this paper.

CRediT authorship contribution statement

M.G. Clerc: Supervision, Project administration, Conceptualization, Methodology, Writing - review & editing. **S. Coulibaly:** Writing - review & editing, Validation. **M.A. Ferré:** Writing - original draft, Writing - review & editing, Software, Investigation, Validation.

Acknowledgments

M.G.C. and M.A.F. are thankful for the financial support of CONICYT-USA, Project No. PII20150011 and Millenium Institute for Research in Optics (MIRO). M.G.C. thanks for the financial support FONDECYT project 1180903. S.C. acknowledge the LABEX CEMPI (ANR-11-LABX-0007) as well as the Ministry of Higher Education and Research, Hauts de France council and European Regional Development Fund (ERDF) through the Contrat de Projets Etat-Region (CPER Photonics for Society P4S).

Supplementary material

Supplementary material associated with this article can be found, in the online version, at doi:10.1016/j.cnsns.2020.105288 .

References

[1] Pikovsky A, Rosenblum M, Kurths J. Synchronization: a universal concept in nonlinear science. Cambridge, England: Cambridge University Press; 2001.
[2] Abrams DM, Strogatz SH. Chimera states for coupled oscillators. Phys Rev Lett 2004;93(17):174102. doi:10.1103/PhysRevLett.93.174102.
[3] Kaneko K. Clustering, coding, switching, hierarchical ordering, and control in a network of chaotic elements. Physica D 1990;41(2):137–72. doi:10.1016/0167-2789(90)90119-A.
[4] Kuramoto Y, Battogtokh D. Coexistence of coherence and incoherence in nonlocally coupled phase oscillators. Nonlin Phenom Complex Syst 2002;5:380–5.
[5] Sethia GC, Sen A, Johnston GL. Amplitude-mediated chimera states. Phys Rev E 2013;88(4):042917. doi:10.1103/PhysRevE.88.042917.

[6] Omel'chenko OE. Coherence-incoherence patterns in a ring of non-locally coupled phase oscillators. Nonlinearity 2013;26(9):2469–98. doi:10.1088/0951-7715/26/9/2469.
[7] Smirnov L, Osipov G, Pikovsky A. Chimera patterns in the Kuramoto–Battogtokh model. J Phys A 2017;50(8):08LT01. doi:10.1088/1751-8121/aa55f1.
[8] Dudkowski D, Maistrenko Y, Kapitaniak T. Different types of chimera states: an interplay between spatial and dynamical chaos. Phys Rev E 2014;90(3):032920. doi:10.1103/PhysRevE.90.032920.
[9] Gopal R, Chandrasekar VK, Venkatesan A, Lakshmanan M. Observation and characterization of chimera states in coupled dynamical systems with nonlocal coupling. Phys Rev E 2014;89(5):052914. doi:10.1103/PhysRevE.89.052914.
[10] Schöll E. Synchronization patterns and chimera states in complex networks: interplay of topology and dynamics. Eur Phys J Spec Top 2016;225:891–919. doi:10.1140/epjst/e2016-02646-3.
[11] Omel'chenko OE, Maistrenko YL, Tass PA. Chimera states: the natural link between coherence and incoherence. Phys Rev Lett 2008;100(4):044105. doi:10.1103/PhysRevLett.100.044105.
[12] Hens CR, Mishra A, Roy PK, Sen A, Dana SK. Chimera states in a population of identical oscillators under planar cross-coupling. Pramana 2015;84:229-235. doi:10.1007/s12043-015-0941-8.
[13] Dudkowski D, Maistrenko Y, Kapitaniak T. Occurrence and stability of chimera states in coupled externally excited oscillators. Chaos 2016;26:116306. doi:10.1063/1.4967386.
[14] Omelchenko I, Omel'chenko OE, Zakharova A, Wolfrum M, Schöll E. Tweezers for chimeras in small networks. Phys Rev Lett 2016;116::114101. doi:10.1103/PhysRevLett.116.114101.
[15] Tumash L, Zakharova A, Lehnert J, Just W, Schöll E. Stability of amplitude chimeras in oscillator networks. EPL 2017;117:20001. doi:10.1209/0295-5075/117/20001.
[16] Omelchenko I, Maistrenko Y, Hövel P, Schöll E. Loss of coherence in dynamical networks: spatial chaos and chimera states. Phys Rev Lett 2011;106:234102. doi:10.1103/PhysRevLett.106.234102.
[17] Omelchenko I, Riemenschneider B, Hövel P, Maistrenko Y, Schöll E. Transition from spatial coherence to incoherence in coupled chaotic systems. Phys Rev E 2012;85:026212. doi:10.1103/PhysRevE.85.026212.
[18] Bogomolov SA, Slepne AV, Strelkova GI, Schöll E, Anishchenko VS. Mechanisms of appearance of amplitude and phase chimera states in ensembles of nonlocally coupled chaotic systems. Commun Nonlin Sci Numer Simul 2017;43:25–36. doi:10.1016/j.cnsns.2016.06.024.
[19] Ujjwal SR, Punetha N, Prasad A, Ramaswamy R. Emergence of chimeras through induced multistability. Phys Rev E 2017;95:032203. doi:10.1103/PhysRevE.95.032203.
[20] Bastidas VM, Omelchenko I, Zakharova A, Schöll E, Brandes T. Quantum signatures of chimera states. Phys Rev E 2015;92(6):062924. doi:10.1103/PhysRevE.92.062924.
[21] Hizanidis J, Kanas VG, Bezerianos A, Bountis T. Existence and control of chimera states in networks of nonlocally coupled models of neuron oscillators. In: Control automation robotics & vision (ICARCV), 2014 13th International conference on. IEEE; 2014. p. 243–6. 10.1109/ICARCV.2014.7064312
[22] Santos M, Szezech J, Borges F, Iarosz K, Caldas I, Batista A, et al. Chimera-like states in a neuronal network model of the cat brain. Chaos Solitons Fract 2017;101:86–91. doi:10.1016/j.chaos.2017.05.028.
[23] Larger L, Penkovsky B, Maistrenko Y. Virtual chimera states for delayed-feedback systems. Phys Rev Lett 2013;111:054103. doi:10.1103/PhysRevLett.111.054103.
[24] Bera BK, Ghosh D. Chimera states in purely local delay-coupled oscillators. Phys Rev E 2016;93:052223. doi:10.1103/PhysRevE.93.052223.
[25] Hizanidis J, Lazarides N, Tsironis GP. Robust chimera states in SQUID metamaterials with local interactions. Phys Rev E 2016;94(3):032219. doi:10.1103/PhysRevE.94.032219.
[26] Tinsley MR, Nkomo S, Showalter K. Chimera and phase-cluster states in populations of coupled chemical oscillators. Nat Phys 2012;8:662–5. doi:10.1038/nphys2371.
[27] Wickramasinghe M, Kiss IZ. Spatially organized dynamical states in chemical oscillator networks: synchronization, dynamical differentiation, and chimera patterns. PLoS ONE 2013;8(11):e80586. doi:10.1371/journal.pone.0080586.
[28] Hart JD, Bansal K, Murphy TE, Roy R. Experimental observation of chimera and cluster states in a minimal globally coupled network. Chaos 2016;26:094801. doi:10.1063/1.4953662.
[29] Hagerstrom AM, Murphy TE, Roy R, Hövel P, Omelchenko I, Schöll E. Experimental observation of chimeras in coupled-map lattices. Nat Phys 2012;8:658–61. doi:10.1038/nphys2372.
[30] Martens EA, Thutupalli S, Fourriére A, Hallatschek O. Chimera states in mechanical oscillator networks. Proc Natl Acad Sci USA 2013;110:10563–7. doi:10.1073/pnas.1302880110.
[31] Kapitaniak T, Kuzma P, Wojewoda J, Czolczynski K, Maistrenko Y. Imperfect chimera states for coupled pendula. Sci Rep 2014;4:6379. doi:10.1038/srep06379.
[32] Rosin DP, Rontani D, Haynes ND, Schöll E, Gauthier DJ. Transient scaling and resurgence of chimera states in networks of boolean phase oscillators. Phys Rev E 2014;90(3):030902. doi:10.1103/PhysRevE.90.030902.
[33] Gambuzza LV, Buscarino A, Chessari S, Fortuna L, Meucci R, Frasca M. Experimental investigation of chimera states with quiescent and synchronous domains in coupled electronic oscillators. Phys Rev E 2014;90:032905. doi:10.1103/PhysRevE.90.032905.
[34] Larger L, Penkovsky B, Maistrenko Y. Laser chimeras as a paradigm for multistable patterns in complex systems. Nat Comm 2015;6:7752. doi:10.1038/ncomms8752.
[35] Uy CH, Weicker L, Rontani D, Sciamanna M. Optical chimera in light polarization. APL Photon 2019;4:056104. doi:10.1063/1.5089714.
[36] Clerc MG, Coulibaly S, Ferré MA, Rojas RG. Chimera states in a duffing oscillators chain coupled to nearest neighbors. Chaos 2018;28:083126. doi:10.1063/1.5025038.
[37] Clerc MG, Coulibaly S, Ferré MA, García-Ñustes MA, Rojas RG. Chimera-type states induced by local coupling. Phys Rev E 2016;93:052204. doi:10.1103/PhysRevE.93.052204.
[38] Clerc MG, Ferré MA, Coulibaly S, Rojas RG, Tlidi M. Chimera-like states in an array of coupled-waveguide resonators. Opt Lett 2017;42:2906–9. doi:10.1364/OL.42.002906.
[39] Peierls RF. The size of a dislocation. Proc Phys Soc 1940;52(34). doi:10.1088/0959-5309/52/1/305.
[40] Nabarro FRN. Dislocations in a simple cubic lattice. Proc Phys Soc 1947;59:256. doi:10.1088/0959-5309/59/2/309.
[41] Clerc MG, Elías RG, Rojas RG. Continuous description of lattice discreteness effects in front propagation. Phil Trans R Soc A 2011;369:412–24. doi:10.1098/rsta.2010.0255.
[42] Kovacic I, Brennan MJ. The Duffing equation: nonlinear oscillators and their behaviour. John Wiley and Sons; 2011.
[43] Ott E. Chaos in dynamical systems. Cambridge, UK: Cambridge University Press; 2002.
[44] Pikovsky A, Politi A. Lyapunov exponents: a tool to explore complex dynamics. Cambridge University Press; 2016.
[45] Skokos C. The Lyapunov characteristic exponents and their computation. Lectures notes physics. Berlin Heidelberg: Springer-Verlag; 2010. Vol. 790;. p. 63–135